

CHANNEL ESTIMATION IN UNDERDETERMINED SYSTEMS UTILIZING VARIATIONAL AUTOENCODERS

Michael Baur, Nurettin Turan, Benedikt Fesl, Wolfgang Utschick

TUM School of Computation, Information and Technology, Technical University of Munich, Germany
Email: {mi.baur, nurettin.turan, benedikt.fesl, utschick}@tum.de

ABSTRACT

In this work, we propose to utilize a variational autoencoder (VAE) for channel estimation (CE) in underdetermined (UD) systems. The basis of the method forms a recently proposed concept in which a VAE is trained on channel state information (CSI) data and used to parameterize an approximation to the mean squared error (MSE)-optimal estimator. The contributions in this work extend the existing framework from fully-determined (FD) to UD systems, which are of high practical relevance. Particularly noteworthy is the extension of the estimator variant, which does not require perfect CSI during its offline training phase. This is a significant advantage compared to most other deep learning (DL)-based CE methods, where perfect CSI during the training phase is a crucial prerequisite. Numerical simulations for hybrid and wideband systems demonstrate the excellent performance of the proposed methods compared to related estimators.

Index Terms— Channel estimation, wideband system, hybrid system, generative model, variational autoencoder.

1. INTRODUCTION

DL has the potential to further enhance future wireless communications systems [1]. For DL, a deep neural network (DNN) is trained on site-specific data to capture prior information about a particular radio propagation environment, which can be leveraged to solve wireless communications-related problems. In various prior work, DL-based methods demonstrate excellent performance in CE [2–6]. In this context, model-based (MB)-DL is an intriguing paradigm for the design of algorithms as it allows combining MB insights with data-based learning [7]. Increased interpretability and a relaxed requirement for training data are two vital aspects MB methods offer for novel algorithm development.

The recently proposed VAE-based channel estimator is a MB-DL method for CE [6, 8]. The basic concept is to

train a VAE on CSI data stemming from a radio propagation environment to learn the underlying channel distribution for which the VAE turns out to be ideally suited. Subsequently, the trained VAE provides input data dependent conditional first and second moments to parameterize an approximation to the MSE-optimal conditional mean estimator (CME). In [6], the authors investigate an uplink (UL) FD multiple-input multiple-output (MIMO) system. UD systems are not covered in [6], but are of high practical relevance. Typical UD instances are hybrid systems with fewer RF chains than antennas [9–12], and wideband systems with time-evolving and frequency-selective channels [13]. Such systems have in common that perfect CSI data necessary for the training of most DL-based methods are not available in real-world applications, apart from elaborate and costly measurement campaigns. In sharp contrast, the VAE-real variant from [6] circumvents this significant drawback of DL-based methods. Its training is solely based on noisy observations from FD systems. However, it is an open question how the VAE-based estimators can be extended for applicability in UD systems.

Contributions: We propose to utilize a VAE for CE in UD systems. We extend the approach from [6] to handle noisy observations stemming from a wide observation matrix, a typical aspect of UD systems. Of particular noteworthiness is the extension of the VAE-real variant, as it requires adapting the training procedure to deal with the information loss caused by the wide observation matrix. The non-trivial extensions in this work make sure that the VAE-real variant preserves its central advantage compared to other DL-based CE algorithms, which is the ability to be trained solely on noisy observations gathered during regular operation at the base station (BS). Simulation results demonstrate the proposed methods' excellent CE performance compared to related estimators.

2. SYSTEM AND CHANNEL MODELS

We assume to receive noisy observations \mathbf{y} of the channel \mathbf{h} as a linear map over a wide observation matrix \mathbf{A} , i.e.,

$$\mathbf{y} = \mathbf{A}\mathbf{h} + \mathbf{n}, \quad \mathbf{A} \in \mathbb{C}^{M \times N}, \quad (1)$$

with $M < N$, $\mathbf{h} \sim p(\mathbf{h})$, and $\mathbf{n} \sim \mathcal{N}_{\mathbb{C}}(\mathbf{0}, \mathbf{\Sigma})$. The matrix \mathbf{A} accounts for the available pilot information. The task

This work is funded by the Bavarian Ministry of Economic Affairs, Regional Development and Energy within the project 6G Future Lab Bavaria. The authors acknowledge the financial support by the Federal Ministry of Education and Research of Germany in the program of “Souverän. Digital. Vernetzt.”. Joint project 6G-life, project identification number: 16KISK002.

in CE is to estimate \mathbf{h} based on \mathbf{y} . Ideally, we would like to evaluate the CME $\mathbb{E}[\mathbf{h} | \mathbf{y}]$, which yields MSE-optimal estimates [14, Ch. 11]. In general, a direct computation of the CME is intractable as it requires access to the unknown distribution $p(\mathbf{h})$ and the solution of an integral over \mathbf{h} , cf. [6]. Another obstacle to performing CE for the system model in (1) is that the matrix \mathbf{A} is wide, which makes the system UD.

2.1. Hybrid System

Let us consider the UL of a single-input multiple-output (SIMO) system, i.e., we have a single-antenna mobile terminal (MT) and a multi-antenna BS. In a hybrid system, the BS has fewer RF chains N_r than receive antennas N_{rx} , and we have $M = N_r$ and $N = N_{rx}$, cf. (1). It is usual to assume that the matrix \mathbf{A} either represents an analog phase-shift network or switches [9–12]. Since we cover the latter partly with the selection matrix in the wideband system model, cf. Section 2.2, we let \mathbf{A} represent a phase-shift network. To this end, \mathbf{A} is realized as a phase-shift matrix with a constant modulus constraint on the matrix elements [12]. A sub-Gaussian matrix comprises these properties and has favorable attributes for sparse recovery problems [15]. More precisely, every entry $A_{i,k}$, $i = 1, \dots, M$, $k = 1, \dots, N$, of \mathbf{A} fulfills $A_{i,k} = \frac{1}{\sqrt{M}} \exp(j\varphi)$, $\varphi \sim \mathcal{U}([0, 2\pi])$.

We assume to have a uniform linear array (ULA) at the BS, which enforces a Toeplitz-structured channel covariance matrix (CCM). For the hybrid system, we make use of CCMs \mathbf{C}_δ that are defined according to a 3rd Generation Partnership Project (3GPP) spatial channel model for an urban macrocell scenario [16]. The spatial channel model computes the CCM as $\mathbf{C}_\delta = \int_{-\pi}^{\pi} g(\vartheta; \delta) \mathbf{a}(\vartheta) \mathbf{a}(\vartheta)^H d\vartheta$, where $g(\vartheta; \delta)$ is an angular power spectrum and $\mathbf{a}(\vartheta)$ is the array steering vector of a ULA. The variable δ comprises information about the path gains and angles of arrival at the BS and follows a prior distribution $p(\delta)$, cf. [4]. We set the propagation cluster number to one in this work. Once the CCM \mathbf{C}_δ is computed, a channel sample is obtained as $\mathbf{h} | \delta \sim \mathcal{N}_{\mathbb{C}}(\mathbf{0}, \mathbf{C}_\delta)$.

2.2. Wideband System

The time-evolution of a frequency-selective single-input single-output (SISO) channel is considered in the wideband system, where $\mathbf{H} \in \mathbb{C}^{N_c \times N_t}$ represents the time-frequency response of the channel with N_c subcarriers and N_t time slots. Let N_p be the number of pilots. The observation matrix is a selection matrix $\mathbf{A} \in \{0, 1\}^{N_p \times N_c N_t}$ with a single one in every row and $\mathbf{h} = \text{vec}(\mathbf{H})$. The ones in \mathbf{A} represent the N_p pilots at the corresponding positions of the $N_c N_t$ channel entries. Thus, we have $M = N_p$ and $N = N_c N_t$, cf. (1).

We generate wideband channels with the QuaDRiGa channel simulator [17]. QuaDRiGa computes the element in the i -th row and j -th column of the channel matrix \mathbf{H} as sum $H_{i,k} = \sum_{\ell=1}^L G_\ell \exp(-2\pi j f_i \tau_{k,\ell})$, $i = 1, \dots, N_c$, $k = 1, \dots, N_t$, over the paths ℓ of in total L multi-paths.

The frequency of subcarrier i is f_i , the delay of path ℓ at time step k is $\tau_{k,\ell}$, and G_ℓ accounts for the path attenuation, antenna radiation pattern, and polarization. We consider an urban macrocell scenario at 2.1 GHz center frequency and 180 kHz bandwidth with $N_c = 12$ and $N_t = 14$, a typical 5G wideband frame [18]. The BS is at 25 m height and covers a 120° sector. The MTs are between 35 and 500 m away from the BS, and are indoors (20 %) and outdoors (80 %). An MT's velocity is uniformly distributed between 0 and 300 km/h.

3. VAE-BASED CHANNEL ESTIMATION

3.1. Preliminaries about the VAE

The elaborations in this section follow the principles of the VAE-based channel estimator in [6]. The evidence-lower bound (ELBO) is the central term for the training of a VAE and is a lower bound to a parameterized likelihood model $p_\theta(\mathbf{h})$ of the unknown channel distribution $p(\mathbf{h})$. An accessible version of the ELBO reads as [19]

$$\mathcal{L}_{\theta, \phi}(\mathbf{h}) = \mathbb{E}_{q_\phi} [\log p_\theta(\mathbf{h} | \mathbf{z})] - \text{D}_{\text{KL}}(q_\phi(\mathbf{z} | \mathbf{y}) \| p(\mathbf{z})) \quad (2)$$

with $\mathbb{E}_{q_\phi(\mathbf{z} | \mathbf{y})}[\cdot] = \mathbb{E}_{q_\phi}[\cdot]$ as the expectation according to the variational distribution $q_\phi(\mathbf{z} | \mathbf{y})$, which depends on the latent vector $\mathbf{z} \in \mathbb{R}^{N_L}$, and is supposed to approximate $p_\theta(\mathbf{z} | \mathbf{h})$. The last term in (2) is the Kullback-Leibler (KL) divergence.

The VAE optimizes the ELBO with the help of DNNs and the reparameterization trick [20]. To this end, it is necessary to define the involved distributions, which we fulfill as follows: $p(\mathbf{z}) = \mathcal{N}(\mathbf{0}, \mathbf{I})$, $p_\theta(\mathbf{h} | \mathbf{z}) = \mathcal{N}_{\mathbb{C}}(\boldsymbol{\mu}_\theta(\mathbf{z}), \mathbf{C}_\theta(\mathbf{z}))$, and $q_\phi(\mathbf{z} | \mathbf{y}) = \mathcal{N}(\boldsymbol{\mu}_\phi(\mathbf{y}), \text{diag}(\boldsymbol{\sigma}_\phi^2(\mathbf{y})))$. Both $p_\theta(\mathbf{h} | \mathbf{z})$ and $q_\phi(\mathbf{z} | \mathbf{y})$ are therefore conditionally Gaussian (CG) distributions, realized by DNNs with parameters θ and ϕ . Accordingly, we obtain closed-form expressions for the terms in (2), i.e., $(-\mathbb{E}_{q_\phi} [\log p_\theta(\mathbf{h} | \mathbf{z})])$ is replaced by the estimate

$$\log \det(\pi \mathbf{C}_\theta(\tilde{\mathbf{z}})) + (\mathbf{h} - \boldsymbol{\mu}_\theta(\tilde{\mathbf{z}}))^H \mathbf{C}_\theta^{-1}(\tilde{\mathbf{z}}) (\mathbf{h} - \boldsymbol{\mu}_\theta(\tilde{\mathbf{z}})), \quad (3)$$

$\tilde{\mathbf{z}} \sim q_\phi(\mathbf{z} | \mathbf{y})$ and $\text{D}_{\text{KL}}(q_\phi(\mathbf{z} | \mathbf{y}) \| p_\theta(\mathbf{z}))$ is the KL divergence between two Gaussian distributions, which has a closed-form expression [6]. A VAE consists of an encoder that represents $q_\phi(\mathbf{z} | \mathbf{y})$ and outputs $\{\boldsymbol{\mu}_\phi(\mathbf{y}), \boldsymbol{\sigma}_\phi(\mathbf{y})\}$ and a decoder that represents $p_\theta(\mathbf{h} | \mathbf{z})$ and outputs $\{\boldsymbol{\mu}_\theta(\mathbf{z}), \mathbf{C}_\theta(\mathbf{z})\}$.

3.2. Fully-Determined Case

The VAE's goal is to compose a CG channel via the latent vector \mathbf{z} such that $\mathbf{h} | \mathbf{z} \sim p_\theta(\mathbf{h} | \mathbf{z})$. As outlined in [6], the law of total expectation allows us to reformulate the CME as

$$\mathbb{E}[\mathbf{h} | \mathbf{y}] = \mathbb{E}_{\mathbf{z}}[\mathbb{E}[\mathbf{h} | \mathbf{z}, \mathbf{y}] | \mathbf{y}]. \quad (4)$$

Under the VAE framework, the inner expectation in (4) exhibits a closed-form solution because the VAE models \mathbf{h} as

CG. The outer expectation is approximated by sampling from $q_\phi(\mathbf{z} | \mathbf{y})$. Let $t_\theta(\mathbf{z}, \mathbf{y}) = \mathbb{E}[\mathbf{h} | \mathbf{z}, \mathbf{y}]$, then $t_\theta(\mathbf{z}, \mathbf{y}) =$

$$\boldsymbol{\mu}_\theta(\mathbf{z}) + \mathbf{C}_\theta(\mathbf{z})\mathbf{A}^H(\mathbf{A}\mathbf{C}_\theta(\mathbf{z})\mathbf{A}^H + \boldsymbol{\Sigma})^{-1}(\mathbf{y} - \mathbf{A}\boldsymbol{\mu}_\theta(\mathbf{z})). \quad (5)$$

If we take one sample $\mathbf{z}^{(1)} = \boldsymbol{\mu}_\phi(\mathbf{y})$ to approximate the outer expectation in (4), we obtain the VAE-based channel estimator from [6]: $\hat{\mathbf{h}}_{\text{VAE}}(\mathbf{y}) = t_\theta(\mathbf{z}^{(1)} = \boldsymbol{\mu}_\phi(\mathbf{y}), \mathbf{y})$. Taking only the single sample $\boldsymbol{\mu}_\phi(\mathbf{y})$ to compute $\hat{\mathbf{h}}_{\text{VAE}}(\mathbf{y})$ achieves excellent CE results for FD systems [6]. The estimator $\hat{\mathbf{h}}_{\text{VAE}}(\mathbf{y})$ is non-linear as a result of the non-linear transformations by the encoder and decoder DNNs, providing $\boldsymbol{\mu}_\theta(\mathbf{z})$ and $\mathbf{C}_\theta(\mathbf{z})$ depending on \mathbf{y} . It is proved in [6] that a VAE-based estimator is theoretically capable of converging to the true CME under certain assumptions. One of the assumptions is that \mathbf{A} is invertible, meaning that the proof does not hold for a wide \mathbf{A} , which motivates the investigation of UD systems.

Among the practicable variants of VAE-based estimators are the VAE-noisy and VAE-real variants [6]. For VAE-noisy, \mathbf{y} is the encoder input, and perfect CSI data \mathbf{h} is available during the training for the computation of (3). VAE-real has only access to \mathbf{y} during the evaluation *and* training. Hence, the ELBO is a lower bound to $p_\theta(\mathbf{y})$ and $p_\theta(\mathbf{h} | \mathbf{z})$ in (2) becomes $p_\theta(\mathbf{y} | \mathbf{z})$ for VAE-real. Consequently, this exchanges \mathbf{h} with \mathbf{y} , $\boldsymbol{\mu}_\theta(\mathbf{z})$ with $\mathbf{A}\boldsymbol{\mu}_\theta(\mathbf{z})$, and $\mathbf{C}_\theta(\mathbf{z})$ with $\mathbf{A}\mathbf{C}_\theta(\mathbf{z})\mathbf{A}^H + \boldsymbol{\Sigma}$ in the expression in (3). Since the decoder outputs $\mathbf{C}_\theta(\mathbf{z})$, the VAE-real variant is still suitable for CE. An intriguing aspect concerning VAE-real is that its training is possible solely based on noisy observations \mathbf{y} , in contrast to the plethora of DL-based channel estimators that require access to perfect CSI data during their training phase. VAE-real can, therefore, be trained at the BS side during regular BS operation, making it a highly realistic estimator.

3.3. Underdetermined Case

In general, if \mathbf{A} is wide, then the linear map $\mathbf{A}\mathbf{h}$ causes a loss of information about \mathbf{h} since a subset of the channels lies in the nullspace of \mathbf{A} . For smaller M , more information is lost, which must be recovered during the training of a potential VAE-based channel estimator. For the VAE-noisy variant, the loss computation is as in (3), since it is assumed that \mathbf{h} is available during the training in this case. Possible simplifications of the loss apply because of the parameterization of $\mathbf{C}_\theta(\mathbf{z})$, discussed at the end of this section. As encoder input for VAE-noisy, we select $\mathbf{A}^H \mathbf{y}$ to obtain an input of the same size as \mathbf{h} . This encoder input does not contain the full information about \mathbf{h} due to the multiplication with \mathbf{A} . Fortunately, the entire information about the ground truth \mathbf{h} is still provided in the loss, which makes it possible that the VAE is capable of inferring a suitable latent representation for \mathbf{h} based on $\mathbf{A}^H \mathbf{y}$ for the estimation task after the training.

The VAE-real variant uses the same encoder input as VAE-noisy. The loss computation is different since only \mathbf{y} is available during the training. The non-invertibility of \mathbf{A}

requires us to calculate (3) directly during the training as the multiplication with \mathbf{A} prevents possible simplifications enabled by $\mathbf{C}_\theta(\mathbf{z})$. However, all the additional computational complexity only affects the offline training procedure. To compensate for the loss of information caused by \mathbf{A} , we propose introducing a changing matrix \mathbf{A} during the training of VAE-real. This way, the VAE can observe the full channel space over the training iterations. For the hybrid system, we do this by sampling a new \mathbf{A} in each iteration. For the wideband system, we place the pilots randomly. After the successful training, VAE-noisy and VAE-real each provide $\boldsymbol{\mu}_\theta(\mathbf{z})$ and $\mathbf{C}_\theta(\mathbf{z})$ to determine the estimate $\hat{\mathbf{h}}_{\text{VAE}}(\mathbf{y})$. What remains is to clarify how $\mathbf{C}_\theta(\mathbf{z})$ is parameterized for the considered system models.

Hybrid System: Since we assume to have a ULA at the BS in the hybrid system, the true CCM is a Toeplitz matrix. A Toeplitz CCM can be asymptotically approximated by a circulant matrix for a large number of antennas [21], which is present in massive MIMO systems. Accordingly, we model the CCM $\mathbf{C}_\theta(\mathbf{z})$ as a circulant matrix. Furthermore, a circulant CCM is diagonalizable by the discrete fourier transform (DFT) matrix $\mathbf{F} \in \mathbb{C}^{N \times N}$ such that $\mathbf{C}_\theta(\mathbf{z}) = \mathbf{F}^H \text{diag}(\mathbf{c}_\theta(\mathbf{z}))\mathbf{F}$, $\mathbf{c} \in \mathbb{R}_+^N$, which implies that we can invert $\mathbf{C}_\theta(\mathbf{z})$ in $\mathcal{O}(N \log N)$ time. As a result, we only need to learn a positive and real-valued vector $\mathbf{c}_\theta(\mathbf{z})$ at the VAE decoder to parameterize a full covariance matrix.

Wideband System: Assuming a constant time-sampling and carrier-spacing, the CCMs along the time- and frequency-axis are each reasonably assumed to be Toeplitz-structured. As $N_t = 14$ and $N_c = 12$, a circulant approximation to each of the CCMs is unfavorable because of the relatively short time and frequency windows. Hence, we model $\mathbf{C}_\theta(\mathbf{z})$ as a block-Toeplitz matrix $\mathbf{C}_\theta(\mathbf{z}) = \mathbf{C}_{\theta,t}(\mathbf{z}) \otimes \mathbf{C}_{\theta,c}(\mathbf{z}) = \mathbf{Q}^H \text{diag}(\mathbf{c}_\theta(\mathbf{z}))\mathbf{Q}$, $\mathbf{c}_\theta(\mathbf{z}) \in \mathbb{R}_+^{4N_c N_t}$, where $\mathbf{C}_{\theta,t}(\mathbf{z})$ represents the Toeplitz CCM along the time axis, and $\mathbf{C}_{\theta,c}(\mathbf{z})$ along the frequency axis. With $\mathbf{Q} = \mathbf{Q}_t \otimes \mathbf{Q}_c$, the matrix $\mathbf{Q}_t \in \mathbb{C}^{2N_t \times 2N_t}$ contains the first N_t columns of the $2N_t \times 2N_t$ DFT matrix, and \mathbf{Q}_c is defined analogously. The matrix \mathbf{Q} , together with $\mathbf{c}_\theta(\mathbf{z})$, defines a positive-definite Hermitian Toeplitz matrix and therefore motivates our parameterization choice for $\mathbf{C}_\theta(\mathbf{z})$ for the wideband system [13].

4. SIMULATION RESULTS

We create a training, validation, and test channel dataset of $T_r = 180,000$, $T_v = 10,000$, and $T_e = 10,000$ samples. We assume that $\boldsymbol{\Sigma} = \zeta^2 \mathbf{I}$ and knowledge of the noise variance ζ^2 during the training and estimation. The channels are normalized in each dataset such that $\mathbb{E}[\|\mathbf{h}\|^2] = N$. Accordingly, we define the signal-to-noise ratio (SNR) as $1/\zeta^2$. We evaluate our methods with the normalized mean squared error (NMSE) $\frac{1}{T_c N} \sum_{i=1}^{T_c} \|\mathbf{h}_i - \hat{\mathbf{h}}_i\|^2$, where \mathbf{h}_i is the i -th test channel realization, and $\hat{\mathbf{h}}_i$ the corresponding estimate. The VAE architectures are almost equivalent to the ones in [6], meaning

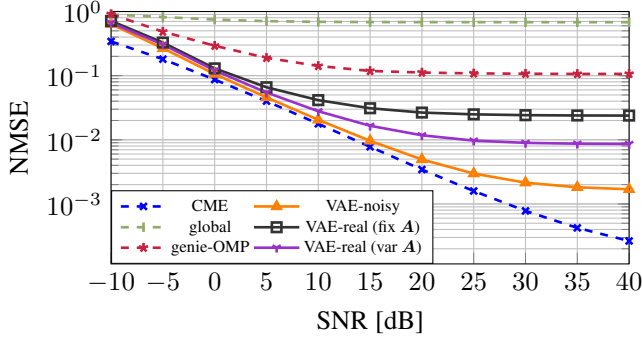


Fig. 1. NMSE over the SNR for the hybrid system from Section 2.1 with $N = 128$ antennas and $N_r = 32$ RF chains.

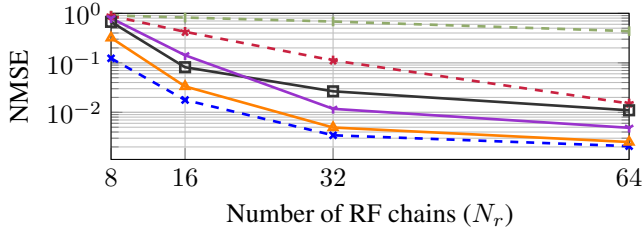


Fig. 2. NMSE over the RF chains for the hybrid system from Section 2.1 with $N = 128$ antennas at an SNR of 20 dB.

we use 1D convolutional layers, batch normalization, ReLU activations, and linear layers to map between dimensions. For a more detailed description, we refer the reader to [6] and the available simulation code¹. The hyperparameters for the architectures were obtained with a random search [22].

We consider the following baseline channel estimators for the hybrid system. As we know the CCM \mathbf{C}_δ in the 3GPP channel model, we can evaluate the CME: $\hat{\mathbf{h}}_{\text{CME}}(\mathbf{y}) = \mathbf{C}_\delta \mathbf{A}^H (\mathbf{A} \mathbf{C}_\delta \mathbf{A}^H + \Sigma)^{-1} \mathbf{y}$. We can also compute a global sample covariance matrix $\hat{\mathbf{C}} = \frac{1}{T_r} \sum_{i=1}^{T_r} \mathbf{h}_i \mathbf{h}_i^H$ from the training dataset channels to evaluate $\hat{\mathbf{h}}_{\text{global}}(\mathbf{y}) = \hat{\mathbf{C}} \mathbf{A}^H (\mathbf{A} \hat{\mathbf{C}} \mathbf{A}^H + \Sigma)^{-1} \mathbf{y}$. Lastly, we also compute an estimate with the orthogonal matching pursuit (OMP) algorithm, a prominent representative from the compressed sensing (CS) literature [10–12]. We utilize a two times oversampled DFT matrix as a dictionary for OMP as a result of the ULA at the BS and use the true channel to determine the sparsity order, which is why we call this estimator genie-OMP.

In Fig. 1, we display the NMSE over the SNR for the hybrid system from Section 2.1 with $N = 128$ antennas and $N_r = 32$ RF chains. It is visible that all estimators, except the CME, exhibit a saturation in the high SNR, which relates to the information loss caused by \mathbf{A} . After the utopian CME, VAE-noisy performs best, followed by VAE-real with a varying \mathbf{A} during the training (purple curve). Consequently, the variation of \mathbf{A} during the training of VAE-real improves the estimation performance. Although genie-OMP uses utopian

¹<https://github.com/baurmichael/vae-est-ud>

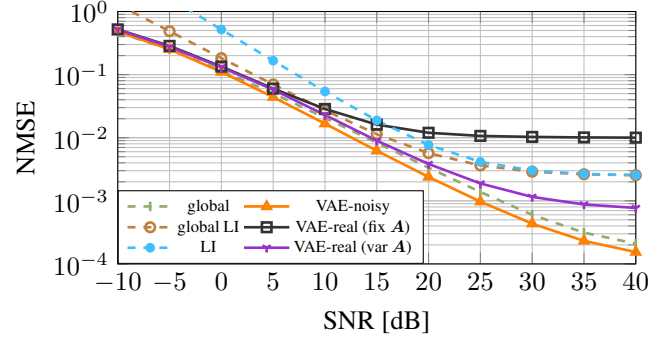


Fig. 3. NMSE over the SNR for the wideband system from Section 2.2 with $N_p = 20$ pilots in lattice layout.

channel knowledge during the estimation, it performs poorly. The $\hat{\mathbf{h}}_{\text{global}}(\mathbf{y})$ estimator performs worst. We illustrate the performance for a varying number of RF chains in Fig. 2 with the same simulation parameters and methods as in Fig. 1. All methods improve in terms of NMSE for increasing N_r . The qualitative order of the methods is as in Fig. 1. Except for $N_r < 32$, the VAE-real with varied \mathbf{A} during the training outperforms the VAE-real with a fixed \mathbf{A} .

At last, in Fig. 3, we show the NMSE over the SNR for the wideband system from Section 2.2 with $N_p = 20$ pilots in lattice layout as described in [13]. For a fair comparison with the VAE-real variants, we display the NMSE for an estimate obtained with linear interpolation (LI) of the missing entries in \mathbf{y} after computing $\mathbf{A}^T \mathbf{y}$. We also compute a sample covariance matrix for the channels from the LI estimates by subtracting the noise covariance from it and truncating the negative eigenvalues to subsequently perform a linear MMSE estimate (global LI) as for $\hat{\mathbf{h}}_{\text{global}}(\mathbf{y})$. All methods that work only with \mathbf{y} saturate in Fig. 3 for high SNR. VAE-noisy shows the best results for all SNR values, followed by the $\hat{\mathbf{h}}_{\text{global}}(\mathbf{y})$ estimator. VAE-real with varying \mathbf{A} during the training outperforms global LI, especially in the high SNR. The performance gap between the two VAE-real variants for high SNR is more prominent in Fig. 3 than in Fig. 1. It seems that varying the selection matrix \mathbf{A} during the training has a more beneficial impact, potentially due to its masking properties.

5. CONCLUSION

This work proposes a VAE-based channel estimator for UD systems. To this end, we analyze hybrid and wideband systems, which are UD systems of high relevance. The VAE-based estimators exhibit superior CE performance compared to the baseline estimators that have equivalent CSI knowledge for the design of the respective estimator. The strong estimation results of the VAE-real variant are particularly noteworthy because VAE-real is trained solely with noisy observations gathered during regular BS operation. We plan to extend the evaluation to measurement data in our future work.

6. REFERENCES

- [1] Emil Björnson, Luca Sanguinetti, Henk Wymeersch, Jakob Hoydis, and Thomas L. Marzetta, “Massive MIMO is a reality—What is next?: Five promising research directions for antenna arrays,” *Digit. Signal Process.*, vol. 94, pp. 3–20, 2019.
- [2] Hao Ye, Geoffrey Y. Li, and Biing-Hwang Juang, “Power of Deep Learning for Channel Estimation and Signal Detection in OFDM Systems,” *IEEE Wirel. Commun. Lett.*, vol. 7, no. 1, pp. 114–117, 2018.
- [3] Mehran Soltani, Vahid Pourahmadi, Ali Mirzaei, and Hamid Sheikhzadeh, “Deep Learning-Based Channel Estimation,” *IEEE Commun. Lett.*, vol. 23, no. 4, pp. 2019–2022, 2019.
- [4] David Neumann, Thomas Wiese, and Wolfgang Utschick, “Learning The MMSE Channel Estimator,” *IEEE Trans. Signal Process.*, vol. 66, no. 11, pp. 2905–2917, 2018.
- [5] Mahdi B. Mashhadi and Deniz Gunduz, “Pruning the Pilots: Deep Learning-Based Pilot Design and Channel Estimation for MIMO-OFDM Systems,” *IEEE Trans. Wirel. Commun.*, vol. 20, no. 10, pp. 6315–6328, 2021.
- [6] Michael Baur, Benedikt Fesl, and Wolfgang Utschick, “Leveraging Variational Autoencoders for Parameterized MMSE Channel Estimation,” *arXiv preprint arXiv:2307.05352*, 2023.
- [7] Nir Shlezinger, Jay Whang, Yonina C. Eldar, and Alexandros G. Dimakis, “Model-Based Deep Learning,” *Proc. IEEE*, vol. 111, no. 5, pp. 465–499, 2023.
- [8] Michael Baur, Benedikt Fesl, Michael Koller, and Wolfgang Utschick, “Variational Autoencoder Leveraged MMSE Channel Estimation,” in *2022 56th Asilomar Conf. Signals, Syst. Comput.*, Pacific Grove, CA, USA, 2022, pp. 527–532, IEEE.
- [9] Khaled Ardah, Gabor Fodor, Yuri C. B. Silva, Walter C. Freitas, and Francisco R. P. Cavalcanti, “A Unifying Design of Hybrid Beamforming Architectures Employing Phase Shifters or Switches,” *IEEE Trans. Veh. Technol.*, vol. 67, no. 11, pp. 11243–11247, 2018.
- [10] Ahmed Alkhateeb, Omar El Ayach, Geert Leus, and Robert W. Heath, “Channel Estimation and Hybrid Precoding for Millimeter Wave Cellular Systems,” *IEEE J. Sel. Top. Signal Process.*, vol. 8, no. 5, pp. 831–846, 2014.
- [11] Roi Mendez-Rial, Cristian Rusu, Nuria Gonzalez-Prelcic, Ahmed Alkhateeb, and Robert W. Heath, “Hybrid MIMO Architectures for Millimeter Wave Communications: Phase Shifters or Switches?,” *IEEE Access*, vol. 4, pp. 247–267, 2016.
- [12] Michael Koller and Wolfgang Utschick, “Learning a compressive sensing matrix with structural constraints via maximum mean discrepancy optimization,” *Signal Processing*, vol. 197, pp. 108553, 2022.
- [13] Benedikt Fesl, Michael Joham, Sha Hu, Michael Koller, Nurettin Turan, and Wolfgang Utschick, “Channel Estimation based on Gaussian Mixture Models with Structured Covariances,” in *2022 56th Asilomar Conf. Signals, Syst. Comput.*, 2022, pp. 533–537.
- [14] Steven M. Kay, *Fundamentals of Statistical Signal Processing: Estimation Theory*, Prentice-Hall, Inc., Englewood Cliffs, NJ, 1993.
- [15] Simon Foucart and Holger Rauhut, *A Mathematical Introduction to Compressive Sensing*, Applied and Numerical Harmonic Analysis. Springer New York, New York, NY, 2013.
- [16] 3GPP, “Spatial channel model for Multiple Input Multiple Output (MIMO) simulations (Release 16),” Tech. Rep. 25.996 V16.0.0, 3rd Generation Partnership Project (3GPP), 2020.
- [17] Stephan Jaeckel, Leszek Raschkowski, Kai Borner, and Lars Thiele, “QuaDRiGa: A 3-D Multi-Cell Channel Model With Time Evolution for Enabling Virtual Field Trials,” *IEEE Trans. Antennas Propag.*, vol. 62, no. 6, pp. 3242–3256, 2014.
- [18] 3GPP, “Physical channels and modulation (Release 17),” Tech. Rep. 38.211 V17.5.0, 3rd Generation Partnership Project (3GPP), 2023.
- [19] Diederik P. Kingma and Max Welling, “An Introduction to Variational Autoencoders,” *Found. Trends® Mach. Learn.*, vol. 12, no. 4, pp. 307–392, 2019.
- [20] Diederik P. Kingma and Max Welling, “Auto-Encoding Variational Bayes,” in *Proc. 2nd Int. Conf. Learn. Represent.*, Banff, Canada, 2014.
- [21] Robert M. Gray, “Toeplitz and Circulant Matrices: A Review,” *Found. Trends® Commun. Inf. Theory*, vol. 2, no. 3, pp. 155–239, 2005.
- [22] James Bergstra and Yoshua Bengio, “Random Search for Hyper-Parameter Optimization,” *J. Mach. Learn. Res.*, vol. 13, no. 10, pp. 281–305, 2012.